Received: 19 July 2019 | Revised: 17 October 2019 | Accepted: 5 November 2019

DOI: 10.1111/vru.12839

ORIGINAL INVESTIGATION

WILEY

Fluorine-18 fluorodeoxyglucose positron emission tomography imaging exhibits increased SUVmax at the level of the spinal intumescence in normal dogs

John M. French[1] | Ariel Brody[2] | Devin von Stade[3] | Chad B. Frank[3] | Lynn R. Griffin[2]

[1]ANTECH Imaging Services, Fountain Valley, California

[2]Department of Environmental and Radiological Health Sciences (ERHS), Colorado State University, Fort Collins, Colorado

[3]Department of Microbiology, Immunology, and Pathology, Veterinary Diagnostic Laboratory, Colorado State University, Fort Collins, Colorado

Correspondence
John M. French, ANTECH Imaging Services Fountain Valley, California.
Email: jmitchellfrench@gmail.com

Abstract

Positron emission tomography (PET) imaging utilizing fluorine-18 labeled fluorodeoxyglucose is a relatively new imaging modality in veterinary medicine that is becoming more common for oncological staging and for musculoskeletal imaging. Thus, it is important to identify the normal variations on PET imaging that may be mistaken for pathology. Variation in standardized uptake values (SUVmax) have been anecdotally identified in the spinal cord of dogs undergoing fluorodeoxyglucose (FDG) PET–CT examinations for oncological staging, with notable increase in SUVmax values identified in the region of the cervical and lumbar spinal intumescences. The aim of this retrospective, analytical study was to compare the SUVmax values at four different locations throughout the spinal cord (C3, C5-T1, T13, and L3-S1) of a group of dogs with no evidence of neurologic disease and compare those findings to histologic specimens from dogs euthanized for unrelated disease. SUVmax values were significantly higher at the cervical and lumbar intumescences in comparison to the control regions ($P < .0001$ and $P < .0001$, respectively). Neuronal count and spinal cord gray matter area were also significantly greater at the cervical and lumbar intumescences (neuronal count $P = .0025$ and $P = .0001$; area $P = .0004$ and $P = .0009$, respectively) while overall neuronal density was lower ($P = .003$ and $P = .028$, respectively). We presume the increased SUVmax values at the spinal cord intumescences are the result of overall increased neuron count, increased proportion of gray matter, and increased spinal cord gray matter area. These findings will aid in the interpretation of future PET–CT studies and hopefully prevent the misdiagnosis of spinal cord disease in normal canines.

KEYWORDS

canine, FDG, PET, spinal cord, spine

1 | INTRODUCTION

Fluorodeoxyglucose (FDG) is a glucose analog that is taken up by metabolically active cells, including cancer cells that have an increased requirement for glucose as an energy substrate to support their uncontrolled growth. For the purposes of imaging, FDG is tagged with the radioactive isotope, fluorine-18 (^{18}F). Fluorine-18 undergoes decay by positron emission, followed by annihilation with an electron and emission of two gamma rays at 180° in opposite directions, allowing for positron emission tomography–CT (PET–CT). This allows for a highly sensitive oncologic imaging for staging, monitoring response to treatment, and assessment for recurrence. Fluorine-18-FDG PET–CT is also used to look for underlying etiology of fever of unknown origin and musculoskeletal imaging as inflammatory cells will also exhibit increased metabolic needs.[1,2]

Fluorine-18-FDG PET–CT is a relatively new imaging modality in veterinary medicine that is becoming increasingly common as more facilities are made available. As ^{18}F-FDG PET–CT is a sensitive but nonspecific imaging tool, it is important for the veterinary diagnostic imaging community to establish what "normal" variants exist in our

Abbreviations: FDG, fluorodeoxyglucose; NeuN, neuronal nuclei; PET, positron emission tomography; ROI, region of interest; SUVmax, maximum standardized uptake value.

EQUATOR network disclosure: The STROBE checklist was used.

Previous publication or presentation disclosure: Findings from this study have not been previously presented or published in an abstract.

[This article was modified on 28 February 2020, after first online publication: "flourodeoxyglucose" replaced to "fluorodeoxyglucose" in the article title.]

[This article was modified on 05 May 2020, after first online publication: "Flourine" replaced to "Fluorine" in the article title.]

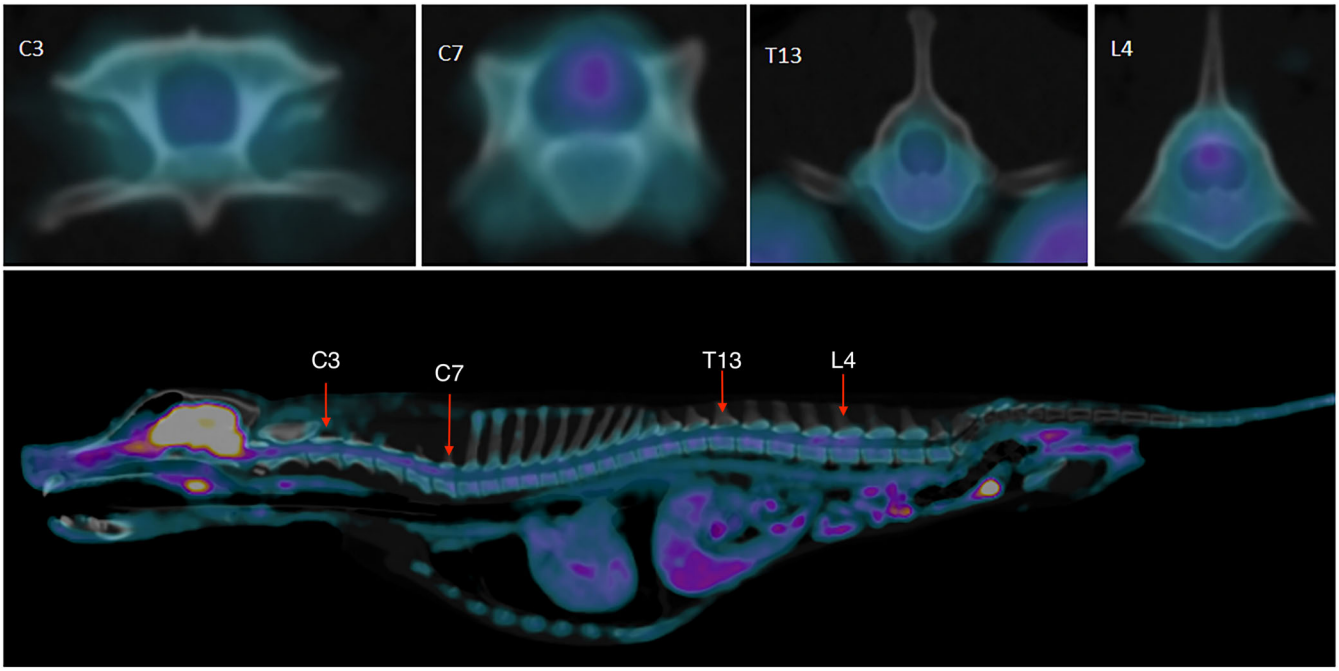

FIGURE 1 Comparative transverse plane fused PET–CT images (window width 350, window length 35) of relative SUVmax at spinal cord segments C3, C7, T13, and L4 and a sagittal plane image of the same dog showing the entire spinal cord. Notice the increased radiopharmaceutical uptake at the level of the cervical and lumbar intumescences [Color figure can be viewed at wileyonlinelibrary.com]

patients. There are many metabolically active tissues in the body that exhibit increased uptake of FDG (avidity). Most of these have been discussed and quantified in a recent paper.[3] Other, more subtle normal variants are harder to elucidate. In particular, we have noticed at this institution that the regions of the cervical and lumbar spinal intumescence consistently exhibit an increase in FDG uptake, resulting in a higher standard uptake value maximum (SUVmax). Standard uptake value is a semiquantitative objective measurement that is used to describe the avidity of a tissue and is reflective of the amount of FDG absorbed by the evaluated tissue. The SUVmax is the maximum voxel SUV within the measured region of interest (ROI). A thorough understanding of all of the normal variants seen on ^{18}F-FDG PET–CT is important for accurate interpretation of these examinations and will prevent misinterpretation of these findings as pathology.

The aim of this study was to evaluate a large number of canine patients undergoing ^{18}F-FDG PET–CT examinations to determine if there is a significant difference in the SUVmax values at different regions of the spinal cord. Specifically, our aim was to compare the SUVmax values at the cervical and lumbar intumescences and compare these values to control regions to determine if there is a difference in SUVmax at the intumescences. We also aimed to compare the neuronal count, neuronal density, and spinal cord area at these same regions to determine if the difference in SUVmax corresponds to a similar difference in any of these variables. The primary hypothesis of this study was that there would be an increased SUVmax in the region of the cervical and lumbar spinal intumescences in comparison to other regions of the spinal cord. The secondary hypothesis was that there would also be an increase in neuronal count, spinal cord area, and neuronal density at these regions.

2 | MATERIALS AND METHODS

This was a retrospective analytical study involving dogs presented to the Colorado State University for ^{18}F-FDG PET–CT examination from November 2009 to June 2016. Dogs with lymphoma, extradural, intradural, or intramedullary spinal cord masses or clinically reported degenerative lower motor neuron disease were excluded from the study. Subject inclusion was determined by consensus between an American College of Veterinary Radiology-certified veterinary radiologist (L.G.) and a third-year diagnostic imaging resident (J.F.).

2.1 | Fluorine-18-FDG PET–CT imaging evaluation

Image assessment was done using a medical imaging viewer (Intellispace Portal version 8, Philips Medical System, Nederland BV). Scans were evaluated by creating a ROI approximately the diameter of the spinal cord on the transverse imaging planes of the CT with an ^{18}F-FDG PET overlay (Figure 1), using a 16-slice PET–CT scanner (Philips Gemini TP Big Bore System; Philips Medical System, Cleveland, OH). Maximum standard uptake values were measured and recorded by ROI analysis on a PET–CT workstation by an independent and non-biased fourth-year veterinary student (A.B.) in the region of the cervical intumescence (C5-T1 vertebral bodies) and lumbar intumescence (L3-S1 vertebral bodies). The recorded SUVmax used for analysis was the highest number visualized in these regions. As a control the cervical intumescence measurement was compared to the SUVmax of the spinal cord as measured over the mid-aspect of the C3 vertebral body and the lumbar intumescence over the mid aspect of the T13 vertebral body. These numbers were recorded and statistical analysis,

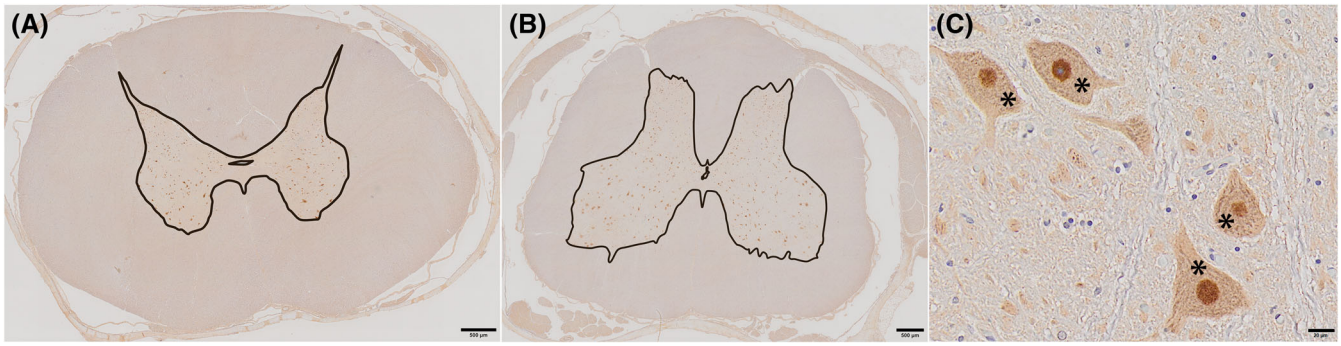

FIGURE 2 A, NeuN stained segment of spinal cord at the level of C3 with gray matter outlined. B, NeuN stained segment of spinal cord at the level of C7 with gray matter outlined. Notice the increased area of gray matter at the level of C7 in comparison to C3. C, NeuN stained segment of spinal cord showing individual neurons (*) that were included in the neuronal count [Color figure can be viewed at wileyonlinelibrary.com]

as outlined below, was performed to determine if there was a significant difference between regions. The observer was given the patient name and medical record number prior to data recording and cases were reviewed in alphabetical order. No additional information was provided at the time of data recording.

2.2 | Histologic evaluation

Histologic evaluation was performed by an American College of Veterinary Pathology-certified veterinary specialist (C.F.) and a first-year veterinary pathology resident (D.V.S.). Spinal cords were collected from two adult dogs following euthanasia for reasons unrelated to central or peripheral nervous system dysfunction. Two sections of spinal cord were collected from segments that corresponded to the C3, C7, T13, and L5 nerve roots, for a total of eight sections from each dog. The sections were routinely processed, sectioned, mounted on a glass slide, and stained with hematoxylin and eosin to confirm the spinal cord was histologically normal and Neuronal nuclei (NeuN; Millipore; MAB377) immunohistochemistry to highlight neuronal soma was used for neuronal quantification. NeuN-stained glass slides were subsequently optically scanned at 200× using a digital microscopy system (Olympus VS120-S5, Olympus Corporation, Tokyo, Japan). A manual count of neuronal cell bodies within the gray matter was performed by a board-certified veterinary pathologist (C.F.) on all sections of spinal cord while viewing the digital images with a photo viewer (Windows Photo Viewer, Microsoft Corporation, Redmond, WA). Neurons were only counted if labeled with NeuN and if the nucleus was in the plane of section (Figure 2). To quantify the total gray matter area in the plane of each spinal cord section (D.V.S.), a bright field microscope (Nikon Eclipse E800, Nikon Corporation, Tokyo, Japan) with a camera (Infinity3 Lumenera, Lumenera Corporation, Ontario, Canada) acquired calibrated images at 200× magnification using image analysis software (Image-pro Premier 64 bit, Media Cybernetics, Rockville, MD) with 135.281 ms exposure with 1.0 gain, 1.0 gamma, and 0 offset. Single image capture was used on some tissue sections, and auto tiling was used on sections of tissue too large to capture the gray matter in a single image. Images were manually examined for accuracy and the gray matter area was measured by digitally tracing using a 455 to 1448 point external polygon and subtracting the area of the central canal (using a 13–97 point polygon tracing).

2.3 | Statistical analysis

Statistical analysis was performed by an American College of Veterinary Surgery-certified veterinary specialist with multiple years of experience performing statistical tests. Categorical variables were summarized with frequencies and percentages. Data normality was assessed using graphical methods, skewness, kurtosis, and Shapiro-Wilk tests. Wilcoxon matched pairs signed-rank tests were performed between variables SUVmax at C3 and SUVmax at C7, and SUVmax at T13 and SUVmax at L5. A paired *t*-test was used to compare neuronal count, area, and neuron density between C3 and C7 and between T13 and L5. Commercially available statistical software (SAS software, Version 9.4 of the SAS System for PC. © 2013 SAS Institute Inc., Cary, NC, USA.; GraphPad Prism for MacIntosh, Version 7, San Diego, CA, USA) was used to perform these analyses and α of .05 was used for statistical significance.

3 | RESULTS

A total of 168 dogs were included in the study. Seventeen dogs had two ^{18}F-FDG PET–CT examinations performed at different time points (median of 3 months between scans, range 0.5-24 months). One dog had 6 ^{18}F-FDG PET–CT examinations performed over the course of 2.5 years, on average every 6 months. A variety of dog breeds were included in the study with the most common being Golden Retriever (28), Labrador Retriever (28), and Mixed breeds (27). Additional dog breeds included Rottweiler (11), Great Pyrenees (10), Great Dane (9), Border Collie (6), Saint Bernard (5), Staffordshire Terrier (5), Bernese Mountain dog (4), German Shepherd (3), Malamute (3), Boxer (2), Doberman Pinscher (2), Greyhound (2), Siberian Husky (2), Mastiff (2), Anatolian Shepherd (1), Australian Shepherd (1), Belgian Malinois (1), Blue Tick Hound (1), Chesapeake Bay Retriever (1), Bulldog (1), English Setter (1), Jack Russell Terrier (1), Mini Schnauzer (1), Newfoundland (1), Old English Sheepdog (1), Shih Tzu (1), and Standard Poodle (1). There were 78 spayed females, two intact females, 76 castrated males,

TABLE 1 Comparative SUVmax values

Site	Median	Interquartile range
C3	1.67	1.41–1.86
C5-T1	2.06[a]	1.76–2.29
T13	1.43	1.24–1.62
L3-S1	1.94[b]	1.71–2.17

[a]C3 versus C5-T1 $P < .0001$.
[b]T13 versus L3-S1 $P < .0001$.

and nine intact males included in the study. The median age of included dogs was 9 years (range 1–14). The average weight of included dogs was 37.4 kg.

All patients underwent ^{18}F-FDG PET–CT imaging with a 16-slice helical PET–CT scanner (Philips Gemini TF Big Bore, Philips North America Corporation, Andover MA) under general anesthesia. Computed tomography technical data were as follows; section collimation thickness of 2 mm, pitch of 0.813, image reconstruction interval of 0 mm, 150 mA and 120 kVp, tube rotation time of 0.5 s, field of view of 600 mm, and a matrix of 768 × 768 mm, with all images reformatted in a standard algorithm. The observer was allowed to manually adjust the window and level. Pre-anesthetic blood glucose levels were obtained just prior to imaging from all patients. No dogs were excluded based on blood glucose values. Anesthesia protocols most commonly involved a combination of an opioid and an alpha-2 agonist, with induction using propofol. Patients were then maintained on an inhalant anesthetic. Once anesthetized, dogs were injected intravenously with 6.29 MBq/kg ^{18}F-FDG and monitored during the 1-h circulation period for the ^{18}F-FDG. Following the 1-h uptake, a whole-body CT scan (pre- and postcontrast) was obtained, immediately followed by whole body PET scan, typically using eight or nine 18.0 cm frames with 1.5-3 min per bed. Computed tomography attenuation-corrected images and non-attenuation-corrected images of the PET data were the reasons for the ^{18}F-FDG PET–CT examination was variable with the majority being performed for cancer staging/screening purposes. The most common primary cancer was osteosarcoma (93; 85 appendicular, 5 axial, 1 parosteal, 1 extraskeletal, 1 radiation induced). Additional cancer types included nasal tumors (17), dermal/subcutaneous mast cell tumor (9), soft tissue sarcoma (6), oral melanoma (3), primary pulmonary neoplasia (3), anal sac adenocarcinoma (2), hemangiosarcoma (2), oral squamous cell carcinoma (2), transitional cell carcinoma (2), acanthomatous ameloblastoma (1), gingival oral fibrosarcoma (1), mammary carcinoma (1), thyroid carcinoma (1), metastatic anaplastic sarcoma (1), and dermal squamous cell carcinoma (1). Seventeen dogs underwent ^{18}F-FDG PET–CT examinations for evaluation of musculoskeletal disease and three dogs due to fever of unknown origin.

The median and interquartile range of all the SUVmax values at each site are reported in Table 1. There was a statistically significant difference in SUVmax values between C3 and C5 ($P < .0001$) and between T13 and L5 ($P < .0001$). The mean neuronal count, gray matter area, and neuronal density of each spinal cord region are reported in Table 2. When comparing neuronal count, area, and neuronal density between the C3 and C7 sites, there was a statistically significant difference between the two sites for all three values ($P = .0025$, .0004, and .003, respectively). When comparing neuronal count, area, and neuronal density between the T13 and L5 regions, there was a statistically significant difference between the two sites for all three values ($P = .0001$, .0009, and .028, respectively). There was a higher neuronal count and larger area associated with both the cervical and lumbar intumescence in comparison to the control areas, and a lower neuronal density.

4 | DISCUSSION

In this study, it has been shown that a statistically significant increase in avidity is present in the region of the cervical and lumbar spinal intumescences. Immunohistochemical staining and quantification of neurons show that this is likely associated with an increase in number of neurons and spinal cord gray matter area in both of these regions. While the neuronal density is actually less than in the control regions, the increased ^{18}F-FDG uptake secondary to overall increased numbers of metabolically active neurons and increased spinal cord area can account for our observation.

Variations in physiologic uptake of FDG throughout the body have been well documented in human medicine[4–6] and have also been investigated in veterinary medicine.[3,7] As ^{18}F-FDG PET imaging becomes more common in veterinary medicine with increasing usage not only for staging of oncology patients but also for musculoskeletal and non-cancer related imaging, it is necessary to understand the normal variations in uptake of FDG. Increased avidity in specific regions within the spinal cord has been documented in the human literature[8–10] and had been anecdotally observed at our institution. The results of the current study indicate this significant difference in SUVmax between spinal cord regions is a normal finding secondary to increased neuronal count and increased spinal cord area.

Fluorodeoxyglucose is a glucose analog that is taken up by metabolically active cells and phosphorylated intracellularly to a form that cannot be further metabolized and thus becomes trapped within the cell. This retention of FDG within the cell results in higher positron emission from regions of higher glucose metabolism that can be characterized using the semi-quantitative SUVmax. The primary physiologic factors contributing to higher SUVmax measurements are numbers of metabolically active cells and rate of metabolic activity of the specific cells within a region of interest. A previous study in rats showed that regions of the spinal cord with increased gray matter content had higher metabolic activity and thus higher FDG uptake compared to regions of the spinal cord with higher white matter content.[10] The highest proportion of gray matter exists from spinal cord segments C6-8 and L4-S1 in people,[10,11] which closely corresponds to the reported cervical (C5-T1) and lumbar intumescence (L2-S3).[12] The proximal cervical segments and the mid thoracic segments that were chosen in this study to be used as control regions have substantially less gray matter.[10] Previous studies in humans have also shown increased FDG uptake in regions of the spinal cord with an increased transverse area, most notably from C3-T2 and L4-S3, which correspond to the reported locations of the cervical and lumbar intumescences.[9]

TABLE 2 Mean neuronal count, neuronal density, and spinal cord area

Site	Mean neuronal count	Mean neuronal density (neurons/mm^2)	Mean spinal cord gray matter area (mm^2)
C3	282 ± 19.8	88.4 ± 7.22	3.195 ± 0.1
C7	493 ± 27.4[a]	54.2 ± 3.26[c]	9.128 ± 0.08[e]
T13	267 ± 13.4	100.9 ± 14.8	2.679 ± 0.32
L5	566 ± 16.9[b]	62.1 ± 5.6[d]	9.160 ± 0.86[f]

[a]C3 versus C7 neuronal count $P = .0025$.
[b]T13 versus L5 neuronal count $P = .0001$.
[c]C3 versus C7 neuronal density $P = .003$.
[d]T13 versus L5 neuronal density $P = .028$.
[e]C3 versus C7 spinal cord gray matter area $P = .0004$.
[f]T13 versus L5 spinal cord gray matter area $P = .0009$.

Our results have shown that there is a statistically significant difference in SUVmax measurements made between the C3 and C7 sites and the T13 and L5 sites in dogs without evidence of neurologic disease. Spinal cord area and neuronal count were also significantly higher at the C7 and L5 sites than at the C3 and T13 sites, respectively. These particular sites were chosen as these regions correspond to the cervical and lumbar intumescences in dogs and were theorized to have an increased density of neurons, a larger spinal cord area, and thus an increased SUVmax. Similar to studies performed in other species the increased SUVmax at these regions is thought to be due to the increased ratio of gray to white matter and the increased overall number of neurons at the cervical and lumbar intumescence.[10]

Interestingly, neuronal density was found to be significantly lower at the C7 and L5 sites when compared to the C3 and T13 sites. This indicates that the overall number of neurons played a larger role than the neuronal density in creating the variability in SUVmax. We propose that the neuronal density had less of an effect on SUVmax because the relative distance between neurons within the spinal cord is far less than the maximum spatial resolution in PET imaging that is in part determined by the positron range of the radionuclide utilized, in this case ^{18}F-FDG. After emission of a positron from an unstable nucleus, there is a finite distance that the positron will travel before undergoing annihilation. This distance is known as the positron range. Positron range is an innate quality of the radionuclide and has been shown to have a mean range of 0.6 mm and a max range as high as 2.4 mm for positrons emitted from ^{18}F-FDG.[13] Both of these values are markedly higher than the observed distance between neurons seen in our study with as many as 100.9 neurons/mm^2 in some locations.

The major limitation of our study was the retrospective nature and lack of histopathologic examination of the spinal cord in enrolled patients at the time of imaging. Instead neurologically normal dogs were used to determine neuronal count, density, and area. While this may not allow for accurate overall values in the patients used for the SUVmax measurements, we presume the overall values are relatively consistent between dogs and more importantly we presume that the relative differences between spinal cord regions will be consistent. The majority of enrolled patients were undergoing oncological staging to evaluate for the potential metastatic disease. Despite the lack of histologic evaluation, it is unlikely that the increased SUVmax within these specific regions of the spinal cord would be the result of metastatic disease for two reasons; one, the increased SUVmax at the C7 and L5 regions was seen consistently at these locations and did not have the variability that would be expected with metastatic disease. And two, in our study, we exempted dogs that had evidence of neurological disease, extradural spinal cord lesions, or cancers that commonly affect or metastasize to the nervous system. This was done to prevent neoplastic or inflammatory cells from influencing our SUVmax measurements. While this does not eliminate the possibility of spinal cord metastases, it decreases the likelihood that patients with metastatic or other spinal cord disease would influence the results.

In conclusion, increased SUVmax at the cervical and lumbar intumescences is a normal variant in canine patients without evidence of neurologic disease. Understanding this normal variation in spinal cord SUVmax will aid in the interpretation of future studies and hopefully prevent the misdiagnosis of spinal cord disease in healthy patients. Future studies investigating the use of ^{18}F-FDG PET–CT in the diagnosis of neoplastic and non-neoplastic spinal cord pathology and the more nuanced variants of ^{18}F-FDG PET–CT imaging are encouraged.

LIST OF AUTHOR CONTRIBUTIONS

Category 1

(a) Conception and Design: French, Griffin
(b) Acquisition of Data: Brody, von Stade, Frank, French, Griffin
(c) Analysis and Interpretation of Data: French, Griffin

Category 2

(a) Drafting the Article: French, Griffin
(b) Revising Article for Intellectual Content: Brody, von Stade, Frank, French, Griffin

Category 3

(a) Final Approval or the Completed Article: Brody, von Stade, Frank, French, Griffin

ACKNOWLEDGEMENTS

The authors would like to thank Brad B. Nelson and Laura Selmic for their assistance with the statistical analysis.

CONFLICT OF INTEREST

The authors declare no potential conflicts of interest with respect to the research authorship, and/or publication of this article.

ORCID

John M. French https://orcid.org/0000-0001-8619-9636
Lynn R. Griffin https://orcid.org/0000-0002-0074-8233

REFERENCES

1. Mann K, Hart J, Duerr F. 18F-FDG positron emission tomography—an innovative technique for the diagnosis of a canine lameness. *Front Vet Sci*. 2016;3:1-6.
2. Kouijzer IJE, Mulders-Manders CM, Bleeker-Rovers CP, Oyen WJG. Fever of unknown origin: The value of FDG-PET/CT. *Semin Nucl Med*. 2018;48:100-107.
3. Randall E, Loeber S, Kraft S. Physiologic variants, benign processes, and artifacts from 106 canine and feline FDG-PET/computed tomography scans. *Vet Radiol Ultrasound*. 2014;55:213-226.
4. Blodgett TM, Fukui MB, Snyderman CH, et al. Combined PET-CT in the head and neck part 1. Physiologic, altered physiologic, and artifactual FDG uptake. *RadioGraphics*. 2005;25:897-912.
5. Ahmad Sarji S. Physiological uptake in FDG PET simulating disease. *Biomed Imaging Interv J*. 2006;2.
6. Shammas A, Lim R, Charron M. Pediatric FDG PET/CT: Physiologic uptake, normal variants, and benign conditions. *RadioGraphics*. 2009;29:1467-1486.
7. Lee MS, Lee AR, Jung MA, et al. Characterization of physiologic ^{18}F-FDG uptake with PET-CT in dogs. *Vet Radiol Ultrasound*. 2010;51:670-673.
8. Bhatt G, Li X-F, Jain A, et al. The normal variant (18)F FDG uptake in the lower thoracic spinal cord segments in cancer patients without CNS malignancy. *Am J Nucl Med Mol Imaging*. 2013;3:317-325.
9. Amin A, Rosenbaum SJ, Bockisch A. Physiological ^{18}F-FDG uptake by the spinal cord: Is it a point of consideration for cancer patients? *J Neurooncol*. 2012;107:609-615.
10. Do BH, Mari C, Tseng JR, Quon A, Rosenberg J, Biswal S. Pattern of ^{18}F-FDG uptake in the spinal cord in patients with non-central nervous system malignancy. *Spine*. 2011;36:1395-1401.
11. Schadrack J, Neto FL, Ableitner A, et al. Metabolic activity changes in the rat spinal cord during adjuvant monoarthritis. *Neuroscience*. 1999;94:595-605.
12. Snyder JM, Hagan CE, Bolon B, Keene CD, *Comparative Anatomy and Histology*. London, UK: Academic Press; 2018. 403-444.
13. Conti M, Eriksson L. Physics of pure and non-pure positron emitters for PET: A review and a discussion. *EJNMMI Phys*. 2016;3:8.

How to cite this article: French JM, Brody A, von Stade D, Frank CB, Griffin LR. Fluorine-18 fluorodeoxyglucose positron emission tomography imaging exhibits increased SUVmax at the level of the spinal intumescence in normal dogs. *Vet Radiol Ultrasound*. 2020;61:364–369. https://doi.org/10.1111/vru.12839